Organic & Biomolecular Chemistry

PAPER

Cite this: *Org. Biomol. Chem.*, 2016, **14**, 2938

A novel pyrimidine tetrad contributing to stabilize tetramolecular G-quadruplex structures†

V. Esposito,[a] A. Pepe,[b] R. Filosa,[c] L. Mayol,[a] A. Virgilio*[a] and A. Galeone*[a]

Received 16th November 2015,
Accepted 5th February 2016

DOI: 10.1039/c5ob02358k

www.rsc.org/obc

G-quadruplex structures formed by oligodeoxyribonucleotides TGGU^{NH_2}GGT (**AM**, U^{NH_2} = 5-amino-2′-deoxyuridine), TGGU^{Br}GGT (**BR**, U^{Br} = 5-bromo-2′-deoxyuridine) and TGGTGGT (**TH**) have been investigated through circular dichroism, nuclear magnetic resonance, gel electrophoresis and molecular modeling techniques. Collected data indicate that all 7-mer oligonucleotides form tetramolecular parallel G-quadruplex structures with all residues adopting *anti* glycosidic bonds. In the case of **AM**, data suggest the occurrence of a novel U^{NH_2}-tetrad characterized by eight hydrogen bonds that stabilizes the G-quadruplex structure more efficiently than U^{Br}- and T-tetrads.

Introduction

DNA duplex has long been considered the main and the most important secondary structure adopted by nucleic acids. However, an increasing amount of investigations in the last 20 years demonstrated that a different DNA secondary structure, namely the G-quadruplex, is also involved in several fundamental biological processes and systems.[1] Apart from their role in molecular biology, G-quadruplex structures are also involved in stabilizing the scaffold of several aptamers endowed with promising pharmaceutical potential[2] and, just as DNA duplex, represent a striking polymeric material for designing and building nanodevices and nanostructures.[3] Both in the case of DNA duplex and G-quadruplex, the applications in nanotechnology depend on their properties of self-recognizing and self-assembling, that rely on the occurrence of base-specific interactions allowing nucleic acid strands to adopt different structures in a controllable manner. From this point of view, the DNA duplex self-assembly depends on the formation of different types of base-pairs, namely the natural Watson–Crick, Hoogsteen, wobble, *etc*. base pairing. On the other hand, the formation of four-stranded structures is mainly based on a remarkably stable four-base arrangement called G-tetrad, while less stable non-G-tetrads formed by canonical nucleobases or mixed tetrads have also been observed.[4]

Notably, among the different types of tetrads, the G-tetrad (and those formed by G analogues) is the only one showing both eight hydrogen bonds linking the four bases together and the precise arrangement of their carbonyls in position 6 required to coordinate a potassium ion sandwiched between two G-tetrads. Although tetrads constituted by the other canonical nucleobases are less stable than G-tetrads, the self-assembly of T-tetrads on a cavitand template in a polar protic solvent has been recently reported.[5] Investigations on such systems could provide useful insight on the role of a non-G-tetrad in nucleic acid topology and stability, and potentially open up new perspectives for the assembly of other unnatural nucleic-acid-based motifs.

A straightforward comparison between the G- and T-tetrads clearly shows a similarity between the arrangement of carbonyls at position 6 in the G-tetrad and that of carbonyls at position 4 in the T-tetrad (Fig. S1, ESI†). The previous consideration and the observation that thymidine, by possessing a carbonyl at position 2, is potentially prone to forming a further hydrogen bond, encouraged us to explore the ability of a non-canonical pyrimidine nucleoside, namely 5-amino-2′-deoxyuridine, to form a more stable tetrad (Fig. 1). In fact, although the amino group at position 5 has a similar size as the methyl group, it is supposedly able to form a hydrogen bond with the carbonyl at position 2. Importantly, this chemical modification is expected not to affect either the 4-carbonyl arrangement required for potassium ion coordination or the hydrogen bonding pattern already observed in T-tetrads, that involves the imino proton (H3) and carbonyl oxygen (O4) of each participating base moiety.[6]

In this frame, the sequence d(TGGU^{NH_2}GGT) (**AM**, in which U^{NH_2} = 5-amino-2′-deoxyuridine) has been prepared and

[a]*Department of Pharmacy, University of Naples "Federico II", Via D. Montesano, 49, 80131 Naples, Italy. E-mail: galeone@unina.it, antonella.virgilio@unina.it; Tel: +39 081678542*
[b]*Department of Science, University of Basilicata, Viale dell'Ateneo Lucano 10, I-85100 Potenza, Italy*
[c]*Department of Experimental Medicine, Second University of Naples, Via Costantinopoli 16, 80138 Napoli, Italy*

†Electronic supplementary information (ESI) available. See DOI: 10.1039/c5ob02358k

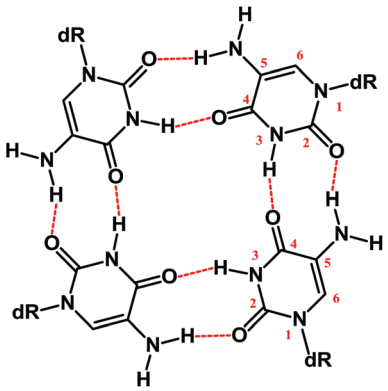

Fig. 1 Hydrogen bonding pattern for a 5-amino-2′-deoxyuridine (U^{NH_2}) tetrad.

Table 1 Sequences investigated and apparent melting temperatures

Name	Sequence (5′-3′)	T_m (°C)	T_m 2 (°C)
AM	d(TGGU^{NH_2}GGT)	70	39
BR	d(TGGU^{Br}GGT)	63	—
TH	d(TGGTGGT)	59	—

investigated by circular dichroism (CD), electrophoresis, NMR and molecular modelling techniques for its ability to form a G-quadruplex structure. Moreover, two further ODNs, namely d(TGGTGGT) (**TH**) and d(TGGU^{Br}GGT) (**BR**), have been analogously investigated to compare the behaviour of the U^{NH_2} residue with the two analogues characterized by similarly sized groups at position 5 (Table 1).

Results and discussion

CD spectroscopy

CD techniques are generally used to assess the presence of G-quadruplex structures and/or to gain preliminary information about their structural features.[7] Fig. 2 shows the CD spectra of the three ODNs investigated (Table 1). Their profiles are all characterized by a negative and a positive band at about 243 and 263 nm, respectively. Since this profile is typical of parallel G-quadruplex structures with all G-residues adopting an *anti* glycosidic conformation, results strongly suggest that **AM**, **BR** and **TH** adopt similar parallel strand arrangements. The general aspect of the CD profiles for all ODNs is not affected by changing the cation concentration (Fig. S2, ESI†). As expected for G-quadruplex structures, signal decrease and increase are clearly observable for lower and higher cation concentrations, respectively. As it is well known, this trend is due to the minor or higher amount of the structured species, whose formation is strongly dependent on the potassium concentration.[8] The G-quadruplex folding was further investigated in sodium buffer. Apart from a decrease in the signal intensity, CD profiles in sodium preserve the main characteristics of

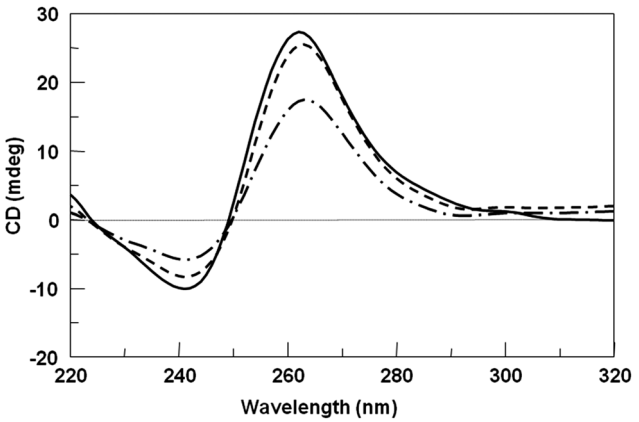

Fig. 2 CD spectra at 20 °C of the investigated G-quadruplex structures at a 100 μM ODN strand concentration in a buffer solution 20 mM KH_2PO_4/K_2HPO_4, 100 mM KCl (pH 7.0). Solid line: **AM**; dashed line: **TH**; dashed-dotted line: **BR**.

those observed in potassium, thus suggesting a similar behavior of the ODNs in the presence of these two types of cations (Fig. S3, ESI†).

NMR spectroscopy

In order to gain more detailed structural information, ODNs **AM**, **BR** and **TH** were investigated by NMR techniques. The ^{1}H-NMR spectra (25 °C, 20 mM KH_2PO_4, 100 mM KCl, 0.2 mM EDTA, pH = 7) for **AM**, **BR** and **TH** (Fig. 3) show the presence of several signals in the diagnostic region of imino protons involved in the G-tetrad formation (between 10.5 and 12.0 ppm), pointing to the presence of G-quadruplex structures

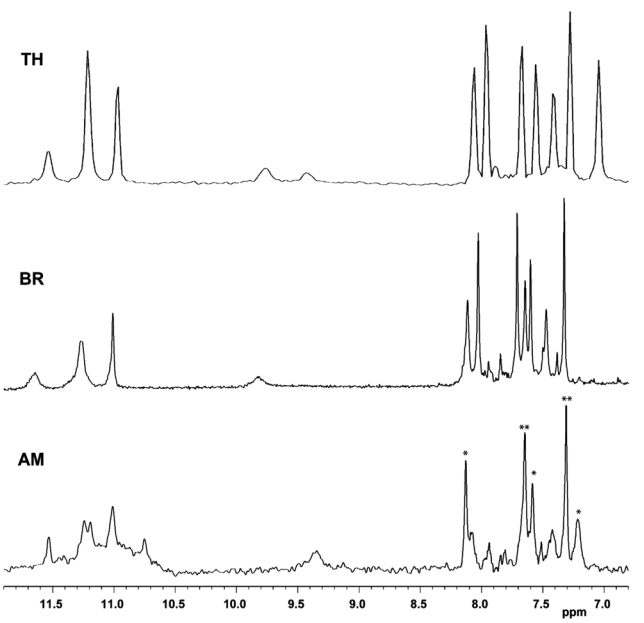

Fig. 3 Imino and aromatic proton regions of the ^{1}H-NMR spectra (500 MHz, T = 25 °C, 20 mM KH_2PO_4, 100 mM KCl, 0.2 mM EDTA, pH = 7) of the investigated G-quadruplex structures.

for all ODNs. Particularly, four NH resonances (two overlapped) in the 10.5–12.0 ppm region are evident in the spectra of **BR** and **TH**, while significantly five signals appear in the same section of the spectrum for **AM**. Taking into account these data, the simple appearance of ^{1}H-NMR spectra of all three ODNs, with seven main singlets in the aromatic region (between 7.0 and 8.2 ppm), indicates that, under the conditions utilized, all the modified oligomers form well-defined hydrogen-bonded major conformations, consistent with highly symmetric G-quadruplex structures containing at least four tetrads and all strands are equivalent and parallel to each other, in agreement with the CD data. With the purpose of obtaining more in depth information about these complexes, the samples have been further investigated by 2D NMR techniques. Their NOESY (Fig. 4, S4 and S5, ESI†) and TOCSY spectra (data not shown) have shown well-dispersed crosspeaks and consequently, both exchangeable and non-exchangeable protons could be nearly completely assigned following the standard procedures (Table S1, ESI†).

Particularly, in the case of **AM**, the further signal at 10.75 ppm in the imino proton region (Fig. 3) could be assigned to 3-NH of the U^{NH_2} residue. As reported for other parallel G-quadruplex structures, the observed NOEs among G-H8 and T-H6 (or U^{Br}- and U^{NH_2}-H6, in the case of **BR** and **AM**, respectively) and their own H1′, H2′ and H2″ ribose protons and the H1′, H2′ and H2″ protons on the 5′-side suggest that all these G-quadruplexes assume a right-handed helical winding. As for the glycosidic torsion angles, for all the G-quadruplex structures formed by the three ODNs investigated, the presence of very weak NOEs between G-H8 (or H6 for T and U analogues) and the corresponding ribose H1′ and of strong NOEs between G-H8 (or H6 for T and U analogues) and ribose H2′ indicates that all nucleosides possess *anti* glycosidic conformations, irrespective of the ODN sequence. On the other hand, as far as the **AM** and **TH** G-quadruplexes are concerned, their NOESY spectra show intense cross peaks between U^{NH_2}4(NH)3 and U^{NH_2}4(NH_2)5 and between T4(NH)3 and T4(CH_3)5, respectively, indicating the formation in both cases of tetrads stabilized by N3–O4 hydrogen bond patterns.[6] Although only this type of hydrogen bond pattern has been observed for U- and T-tetrads both in NMR[6,9] and X-ray[10] investigations, a N3–O2 pattern would be theoretically possible for these types of tetrads, as well as for the U^{NH_2}-tetrad. However, in the latter case, the NH_2 group would lie into the grove without the possibility to form an extra hydrogen bond and, furthermore, the observed NOE between U^{NH_2}4(NH)3 and U^{NH_2}4(NH_2)5 would not be compatible with this tetrad arrangement. A further possibility that we have considered, namely the formation of two U^{NH_2}–U^{NH_2} base pairs, has been straightforwardly excluded due to the strand equivalence observed. The chemical shifts observed for U^{NH_2}4H6 (**AM**) and T4H6 (**TH**) (Table S1, ESI†) are in agreement with those reported for T- and U-tetrads,[6,9] taking into account the differences concerning the substituent at position 5, the residue position in the sequence, and the buffer and temperature conditions used in the cited studies. The observed NOEs of U^{NH_2}4H6 with G5H8 and G3H8 suggest that the U^{NH_2}-tetrad is well sandwiched between the two G-tetrads adjacent to it (data not shown).

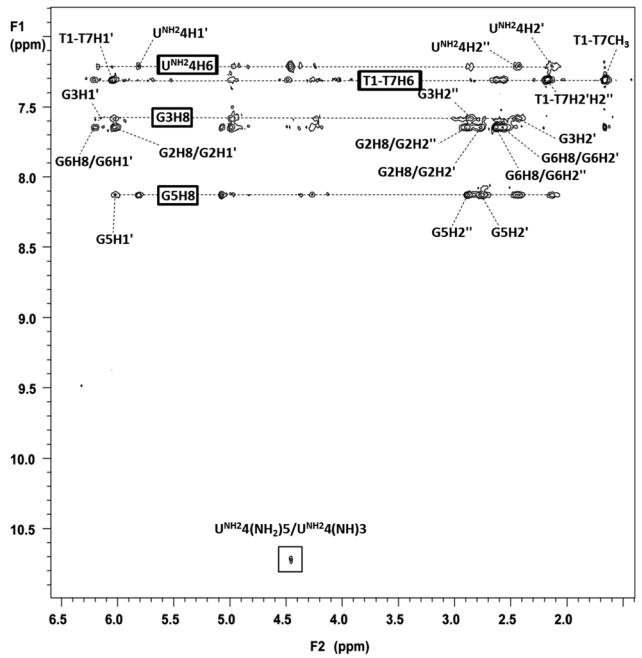

Fig. 4 Expanded region of the 2D NOESY spectrum of G-quadruplex **AM** (500 MHz; 25 °C; strand concentration 1.5 mM; 20 mM KH_2PO_4/K_2HPO_4, 100 mM KCl and 0.2 mM EDTA, pH 7.0 in H_2O/D_2O 9 : 1; total volume 0.6 ml; mixing time 180 ms) correlating bases H8/H6 and sugar protons. The box identifies the NOE between U^{NH_2}4(NH)3 and U^{NH_2}4-(NH_2)5. See the text for details.

In the case of **AM**, the proton decoupled phosphorus spectrum under buffer conditions at 25 °C has been acquired (Fig. S6, ESI†). Data show that all ^{31}P signals are clustered within the −0.8 and −2.2 ppm region, characteristic of unperturbed backbone phosphates of parallel stranded G-quadruplex structures.[11]

It should be noted that, at least from a theoretical point of view, the four strands in a tetramolecular G-quadruplex structure, could arrange in topologies different from the parallel one, namely into two different antiparallel arrangements and a mixed parallel–antiparallel arrangement (sometimes called 3 + 1).[12] However, in these cases, guanosines adopting *syn* glycosidic conformations should be observed,[13] the strands should not be equivalent for symmetry reasons and the expected number of signals should be higher than that observed for **TH**, **BR** and for the major structure of **AM**. Nevertheless, in the latter case, the NMR data have not allowed us to rule out the presence of very minor species not adopting the parallel arrangements.

CD melting and gel electrophoresis

CD melting and annealing experiments were recorded for all the G-quadruplex structures formed by **AM**, **BR** and **TH**. As expected for tetramolecular G-quadruplex structures, melting and annealing profiles (Fig. 5 and S7, ESI,† respectively) show an evident hysteresis under the experimental conditions used.[8] However the apparent melting temperatures[14] inferred

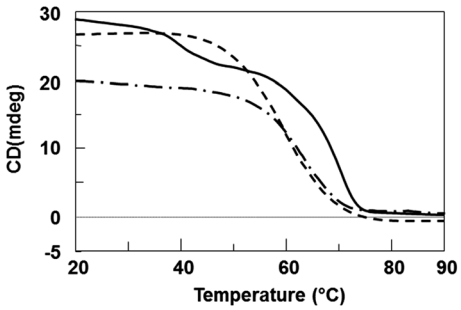

Fig. 5 CD melting curves registered as a function of temperature for all G-quadruplex structures at their maximum Cotton effect wavelengths. CD data were recorded in a 0.1 cm pathlength cuvette at a scan rate of 10 °C h^{-1} at a 100 μM ODN strand concentration in K^+ buffer. Solid line: **AM**; dashed line: **TH**; dashed-dotted line: **BR**.

by melting profiles have been useful to evaluate the relative thermal stability of the G-quadruplex structures formed by **AM**, **BR** and **TH**. Collected data (Table 1) indicate the following stability trend **AM** > **BR** > **TH**, thus suggesting a more important contribution to the structural stability of the U^{NH_2}-tetrad, compared to the U^{Br}- and T-tetrad. Remarkably, the CD melting profile of **AM** shows a further inflection point at about 39 °C. In a recent paper,[15] studies regarding some natural ODNs similar to those here investigated (general sequence XGGYGGT, where X and Y are A, T, C or G), have been reported. Particularly, the d(TGGAGGT) G-quadruplex showed a CD melting profile with two inflection points and PAGE data suggested the formation of dimeric species (two 5′-5′ end-stacked G-quadruplexes, according to the authors proposal). Although the authors clearly showed that the biphasic CD melting profile of the d(TGGAGGT) G-quadruplex was not correlated with the formation of higher order structures, in order to verify this possibility for our sequences also, we analyzed them by PAGE. Results showed that **AM**, **BR**, and **TH** form G-quadruplex structures with electrophoretic motilities very similar to each other and to the tetramolecular G-quadruplex structure formed by TG_5T used as a reference[8] (Fig. S8, ESI†). This datum indicates the occurrence of tetramolecular strand arrangements for **AM**, **BR**, and **TH**, in agreement with results obtained by NMR investigations. In particular, no evidence for dimeric species could be observed in the case of **AM**, although it was run at different ODN concentrations. Since the transition at 39 °C in the CD profile could not be ascribed to an equilibrium monomer–dimer, we tentatively propose a behavior similar to that hypothesized in the case of the d(TGGAGGT) G-quadruplex for which a not totally cooperative melting process was suggested.[15]

Molecular modelling

According to NMR data we built molecular models of G-quadruplex structures of **AM**, **BR** and **TH** (Fig. 6, S9 and S10, ESI,† respectively), as described in the Experimental section. As expected, the structures show a right-handed helical backbone geometry, in which the four strands are equivalent to each other and all nucleosides adopt *anti* glycosidic conformations. In particular, it should be noted that, not only all purine bases involved in the formation of G-tetrads, but also the pyrimidine residues U^{NH_2}, U^{Br} and T, are able to form well-defined and planar tetrads without causing any distortions of the backbone and result in a good stacking with the adjacent G-tetrads.

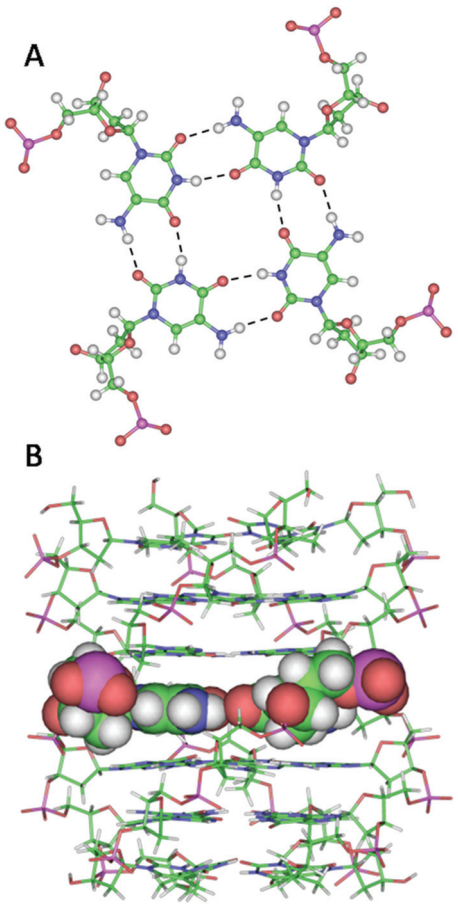

Fig. 6 (A) Ball and stick model of the U^{NH_2}-tetrad observed in the G-quadruplex structure of **AM**. Dashed black lines represent hydrogen bonds. (B) Side view of stick model of G-quadruplex structure adopted by **AM**. The U^{NH_2}-tetrad is reported in CPK. Heavy atoms are shown with different colors (carbons, green; nitrogens, blue; oxygens, red; hydrogens, white; phosphorus, purple).

Nevertheless, according to NMR data concerning U^{NH_2} residues, it is interesting to note the formation of a further hydrogen bond between the NH_2 group at position 5 and the carbonyl one at position 2, in addition to the N3–O4 hydrogen bonds. However, as far as the **BR** G-quadruplex is concerned, the U^{Br}-tetrad appears to be slightly wider than those formed by the other two analogues, as a result being partially more accessible to the solvent.

Conclusions

The presence of an additional hydrogen bond donor (namely, the amino group) in the pyrimidine derivative 5-amino-2′-deoxy-

uridine endows this modified nucleoside with a further side, by which its ability to recognize other nucleotides could be remarkably increased. This property has been already exploited in the molecular recognition based on a DNA triple helix.[16] In fact, 5-amino-2′-deoxyuridine, when present in the triplex central strand, is able to recognize all the four natural nucleotides in the third strand, depending on the strand orientation. In this paper we show that 5-amino-2′-deoxyuridine is also able to form a tetrad stabilized by eight hydrogen bonds which, to the best of our knowledge, is the first pyrimidine tetrad investigated showing this characteristic. Recent reports have highlighted that G-quadruplex structures have been adopted by several aptamers[17] which are nucleic acid ligands for specific targets, selected from random oligonucleotide libraries through a technique called SELEX.[18] In advanced versions of this technique, more promiscuous engineered DNA polymerases have been exploited, with the aim to incorporate chemically modified nucleotides also in the initial library and, then, expand the structural repertoire. In this frame, 5-amino-2′-deoxyuridine can be considered a suitable modified nucleotide for the following reasons: (1) the ability to form a base-pair with adenine is preserved, this property being essential for the amplification step in SELEX techniques; (2) the extra amino-group is potentially able to form both hydrogen and ionic bonds with the target, depending on the conditions used in the selection steps; (3) 5-amino-2′-deoxyuridine residues are able to form quite stable tetrads. The self-assembly properties of G-quadruplex structures and then, their potential applications, could benefit from the implementation of new structural motifs. Furthermore, the importance of non-G tetrads in synthetic template-assembled systems has been recently highlighted.[5,19]

Further investigations concerning the occurrence of U^{NH_2}-tetrads in other different sequence contexts and in non-aqueous environments have been planned in our laboratory.

Experimental section

Oligonucleotide synthesis and purification

The modified oligonucleotides reported in Table 1 were synthesized on a Millipore Cyclone Plus DNA synthesizer using solid phase β-cyanoethyl phosphoramidite chemistry at the 15 μmol scale. The synthesis of the suitably protected 5-amino-2′-deoxyuridine-3′-phosphoramidite was performed following the synthetic strategy proposed by Barawkar and Ganesh.[20] 5-Bromo-2′-deoxyuridine-3′-phosphoramidite was purchased from Glen Research. The oligomers were detached from the support and deprotected by treatment with concentrated aqueous ammonia at 55 °C overnight (**AM** and **TH**) or at room temperature for 24 h (**BR**). The combined filtrates and washings were concentrated under reduced pressure, redissolved in H_2O, analyzed and purified by high-performance liquid chromatography on a Nucleogel SAX column (Macherey-Nagel, 1000-8/46), using buffer A: 20 mM KH_2PO_4/K_2HPO_4 aqueous solution (pH 7.0) containing 20% (v/v) CH_3CN and buffer B: 1 M KCl, 20 mM KH_2PO_4/K_2HPO_4 aqueous solution (pH 7.0) containing 20% (v/v) CH_3CN; a linear gradient from 0 to 100% B for 30 min and a flow rate of 1 ml min^{-1} were used. The fractions of the oligomers were collected and successively desalted by Sep-pak cartridges (C-18). The isolated oligomers proved to be >98% pure by NMR (Fig. S11 and S12, ESI†).

CD spectroscopy

CD samples of oligonucleotides reported in Table 1 were prepared at a concentration of 1×10^{-4} M by using potassium buffer solutions (20 mM KH_2PO_4/K_2HPO_4 supplemented with different KCl concentrations, namely 10, 100 and 300 mM, pH 7.0) or a sodium buffer solution (20 mM NaH_2PO_4/Na_2HPO_4, 100 mM NaCl, pH 7.0). CD spectra of all G-quadruplexes and CD melting/annealing curves were registered on a Jasco 715 CD spectrophotometer. For the CD spectra, the wavelength was varied from 220 to 320 nm at a 100 nm min^{-1} scan rate, and the spectra were recorded with a response of 16 s, at 2.0 nm bandwidth and normalized by subtraction of the background scan with the buffer. The temperature was kept constant at 20 °C with a thermo-electrically-controlled cell holder (Jasco PTC-348). CD melting/annealing curves were registered as a function of temperature (range: 20 °C–90 °C) for all G-quadruplexes at their maximum Cotton effect wavelengths. The CD data were recorded in a 0.1 cm pathlength cuvette at a scan rate of 10 °C h^{-1}.

NMR spectroscopy

NMR samples were prepared at a concentration of about 1.5 mM, in 0.6 mL (H_2O/D_2O 9 : 1 v/v) buffer solution having 20 mM KH_2PO_4, 100 mM KCl, 0.2 mM EDTA, pH = 7. All the samples were heated for 5–10 min at 80 °C and slowly cooled (10–12 h) to room temperature. The solutions were equilibrated for several weeks at 4 °C. The annealing process was assumed to be complete when ^{1}H NMR spectra were superimposable on changing the time. NMR spectra were recorded with a Varian Unity INOVA 500 MHz spectrometer. 1D proton spectra of the sample in H_2O were recorded using the pulsed-field gradient DPFGSE for H_2O suppression. ^{1}H-chemical shifts were referenced relative to external sodium 2,2-dimethyl-2-silapentane-5-sulfonate (DSS). The pulsed-field gradient DPFGSE sequence was used for NOESY (180 ms and 80 ms mixing times) and TOCSY (120 ms mixing time) experiments in H_2O. All experiments were recorded using the States-TPPI procedure for quadrature detection. In all 2D experiments, the time domain data consisted of 2048 complex points in t2 and 400–512 fids in the t1 dimension. A relaxation delay of 1.2 s was used for all experiments.

The proton decoupled phosphorus spectra were acquired under the same conditions as the ^{1}H NMR ones at 25 °C with a Varian Unity INOVA 500 MHz spectrometer. ^{31}P-chemical shifts were referenced relative to external phosphoric acid (H_3PO_4 85% v/v).

Gel electrophoresis

All oligonucleotides were analyzed by non-denaturing PAGE. Samples annealed in the NMR buffer (20 mM KH_2PO_4,

100 mM KCl, 0.2 mM EDTA, pH = 7; [ODN] ≈ 0.5–1.5 mM) were loaded on a 16% polyacrylamide gel containing Tris-Borate-EDTA (TBE) 2.5× and KCl 30 mM. The run buffer was TBE 1× containing 100 mM KCl. For all samples, a solution of glycerol/TBE 10× containing 100 mM KCl (2 : 1) was added just before loading. Electrophoresis was performed at 8 V cm^{-1} at room temperature. Bands were visualized by UV shadowing.

Molecular modeling

The main conformational features of G-quadruplexes **AM**, **BR** and **TH** were explored by means of a molecular modelling study. The AMBER force field using the AMBER 99 parameter set was used. In all three cases, the initial coordinates for the starting models of the quadruplexes were taken from the NMR solution structure of the quadruplex $[d(TGGTGGC)]_4$ (Protein Data Bank entry number 1EMQ), having a structure with the lowest energy. The complete structures of the modified G-quadruplexes were then built using the Biopolymer building tool of Discover. The initial $[d(TGGTGGT)]_4$ G-quadruplex model was built by deleting the cytosine base at the 3′-end and by replacing it with a thymine one in each of the four d(TGGTGGC) strands. The $[d(TGGU^{NH_2}GGT)]_4$ and $[d(TGGU^{Br}GGT)]_4$ models instead were obtained from the $[d(TGGTGGT)]_4$ one by removing the methyl group at position 5 of T4 residues and replacing it with an amino one or a bromine atom, respectively. The calculations were performed using a distance-dependent macroscopic dielectric constant of 4*r*, and an infinite cut-off for non-bonded interactions to partially compensate for the lack of a solvent.[21] Using the steepest descent followed by the quasi-Newton Raphson method (VA09A), the conformational energy of each complex was minimized until convergence to an RMS gradient of 0.1 kcal mol^{-1} $Å^{-1}$ was reached. Illustrations of structures were generated using the INSIGHT II program, version 2005 (Accelrys, San Diego, CA, USA). All the calculations were performed on a PC running Linux ES 2.6.9.

Acknowledgements

We thank the Regione Campania under POR Campania FESR 2007–2013 – O.O. 2.1 (FarmaBioNet) for financial support.

References

1 D. Rhodes and H. J. Lipps, *Nucleic Acids Res.*, 2015, **18**, 8627.
2 V. Viglasky and T. Hianik, *Gen. Physiol. Biophys.*, 2013, **32**, 149.
3 L. A. Yatsunyk, O. Mendoza and J.-L. Mergny, *Acc. Chem. Res.*, 2014, **47**, 1836 and references cited therein.
4 For recent examples see: (*a*) A. Virgilio, V. Esposito, G. Citarella, L. Mayol and A. Galeone, *ChemBioChem*, 2012, **13**, 2219; (*b*) P. Šket and J. Plavec, *J. Am. Chem. Soc.*, 2010, **132**, 12724; (*c*) N. S. Bhavesh, P. K. Patel, S. Karthikeyan and R. V. Hosur, *Biochem. Biophys. Res. Commun.*, 2004, **317**, 625; (*d*) K. W. Lim, P. Alberti, A. Guédin, L. Lacroix, J.-F. Riou, N. J. Royle, J.-L. Mergny and A. T. Phan, *Nucleic Acids Res.*, 2009, **37**, 6239, and references cited therein.
5 (*a*) W.-Q. B. Hui and J. C. Sherman, *Tetrahedron Lett.*, 2014, **55**, 1479; (*b*) G. A. L. Bare and J. C. Sherman, *J. Org. Chem.*, 2013, **78**, 8198.
6 P. K. Patel and R. V. Hosur, *Nucleic Acids Res.*, 1999, **27**, 2457.
7 M. Vorlíčková, I. Kejnovská, J. Sagi, D. Renčiuk, K. Bednářová, J. Motlová and J. Kypr, *Methods*, 2012, **57**, 64.
8 J. Gros, F. Rosu, S. Amrane, A. De Cian, V. Gabelica, L. Lacroix and J.-L. Mergny, *Nucleic Acids Res.*, 2007, **35**, 3064.
9 (*a*) C. Cheong and P. B. Moore, *Biochemistry*, 1992, **31**, 8406; (*b*) Y. Xu, T. Ishizuka, T. Kimura and M. Komiyama, *J. Am. Chem. Soc.*, 2010, **132**, 7231.
10 (*a*) J. Deng, Y. Xiong and M. Sundaralingam, *Proc. Natl. Acad. Sci. U. S. A.*, 2001, **98**, 13665; (*b*) B. Pan, Y. Xiong, K. Shi and M. Sundaralingam, *Structures*, 2003, **11**, 1423.
11 (*a*) S. S. Wijmenga and B. N. M. van Buuren, *Prog. Nucl. Magn. Reson. Spectrosc.*, 1998, **32**, 287; (*b*) D. G. Gorenstein, *Phosphorus-31 NMR: Principles and Applications*, Academic Press, New York, 1984; (*c*) V. A. Roongta, C. R. Jones and D. G. Gorenstein, *Biochemistry*, 1990, **29**, 5245.
12 V. Esposito, A. Galeone, L. Mayol, G. Oliviero, A. Virgilio and L. Randazzo, *Nucleosides, Nucleotides Nucleic Acids*, 2007, **26**, 1155.
13 A. Virgilio, V. Esposito, G. Citarella, A. Pepe, L. Mayol and A. Galeone, *Nucleic Acids Res.*, 2012, **40**, 461.
14 J.-L. Mergny, A. De Cian, A. Ghelab, B. Saccà and L. Lacroix, *Nucleic Acids Res.*, 2005, **33**, 81.
15 V. D'Atri, N. Borbone, J. Amato, V. Gabelica, S. D'Errico, G. Piccialli, L. Mayol and G. Oliviero, *Biochimie*, 2013, **99**, 119.
16 (*a*) V. S. Rana, D. A. Barawkar and K. N. Ganesh, *J. Org. Chem.*, 1996, **61**, 3578; (*b*) V. S. Rana and K. N. Ganesh, *Org. Lett.*, 1999, **1**, 631.
17 W. O. Tucker, K. T. Shum and J. A. Tanner, *Curr. Pharm. Des.*, 2012, **18**, 2014.
18 M. Darmostuk, S. Rimpelova, H. Gbelcova and T. Ruml, *Biotechnol. Adv.*, 2015, **33**, 1141.
19 (*a*) W.-Q. B. Hui and J. C. Sherman, *ChemBioChem*, 2012, **13**, 1865; (*b*) W.-Q. B. Hui and J. C. Sherman, *Chem. Commun.*, 2012, **48**, 109.
20 D. Barawkar and K. N. Ganesh, *Bioorg. Med. Chem. Lett.*, 1993, **3**, 347.
21 S. J. Weiner, P. A. Kollman, D. A. Case, U. C. Singh, C. Ghio, G. Alagona, S. Profeta and P. J. Weiner, *J. Am. Chem. Soc.*, 1984, **106**, 765.